Submitted to Chemical Physics Letters

UCRL-19192
Preprint

c. 2

OPTICALLY DETECTED ^{35}Cl AND ^{37}Cl HYPERFINE AND NUCLEAR QUADRUPOLE INTERACTIONS IN EXCITED TRIPLET STATES IN ZERO FIELD

M. J. Buckely and C. B. Harris

RECEIVED
LA...
RADIATION LABORATORY
APR 15 1970
LIBRARY AND
DOCUMENTS SECTION

February 1970

AEC Contract No. W-7405-eng-48

TWO-WEEK LOAN COPY

This is a Library Circulating Copy which may be borrowed for two weeks. For a personal retention copy, call Tech. Info. Division, Ext. 5545

LAWRENCE RADIATION LABORATORY
UNIVERSITY of CALIFORNIA BERKELEY

UCRL-19192

DISCLAIMER

This document was prepared as an account of work sponsored by the United States Government. While this document is believed to contain correct information, neither the United States Government nor any agency thereof, nor the Regents of the University of California, nor any of their employees, makes any warranty, express or implied, or assumes any legal responsibility for the accuracy, completeness, or usefulness of any information, apparatus, product, or process disclosed, or represents that its use would not infringe privately owned rights. Reference herein to any specific commercial product, process, or service by its trade name, trademark, manufacturer, or otherwise, does not necessarily constitute or imply its endorsement, recommendation, or favoring by the United States Government or any agency thereof, or the Regents of the University of California. The views and opinions of authors expressed herein do not necessarily state or reflect those of the United States Government or any agency thereof or the Regents of the University of California.

Submitted to Chemical Physics Letters

UCRL-19192
Preprint

UNIVERSITY OF CALIFORNIA

Lawrence Radiation Laboratory
Berkeley, California

AEC Contract No. W-7405-eng-48

Optically Detected ^{35}Cl and ^{37}Cl Hyperfine and Nuclear Quadrupole Interactions in Excited Triplet States in Zero Field

M. J. Buckely and C. B. Harris

February, 1970

Optically Detected ^{35}Cl and ^{37}Cl Hyperfine and Nuclear Quadrupole Interactions in Excited Triplet States in Zero Field

M. J. Buckley and C. B. Harris*

Department of Chemistry, University of California,
and the Inorganic Materials Research Division,
Lawrence Radiation Laboratory,
Berkeley, California 94720

Abstract

The zero field optical detection of the electron spin resonance and Cl ENDOR of 8-chloroquinoline in its $^3(\pi,\pi^*)$ state is reported. The observed data is interpreted in terms of a spin-Hamiltonian which includes the ^{14}N, ^{35}Cl, and ^{37}Cl nuclear-electron hyperfine and nuclear quadrupole interactions. Values for these parameters are obtained for the excited triplet state.

* To whom correspondence should be addressed.

Introduction

Optical detection of electron spin resonance in zero field of azaaromatic $^3(\pi,\pi^*)$ states was first reported by Schmidt and van der Waals[1] and later by Tinti, El-Sayed, Maki, and Harris[2] for quinoxaline and 2,3 dichloroquinoxaline, respectively. The accompanying zero field optically detected ENDOR was reported by Harris, et al[3], and subsequently by Chan, Schmidt and van der Waals[4]. The effect of the nitrogen nuclear quadrupole interaction and electron-nitrogen hyperfine interaction in the interpretation of the ENDOR has been given by Buckley, Harris, and Maki[5] in terms of the electron-magnetic dipole moment transition operator. On this basis the ^{14}N nuclear quadrupole interaction, $\nu_- = 3e^2qQ(1 - \eta/3)/4$, for the $^3(\pi,\pi^*)$ state of quinoline[5], quinoxaline[5], and 2,3 dichloroquinoxaline[3] has been obtained. In addition, the interpretation of the structure seen in zero field electron spin resonance has provided values for the ^{14}N hyperfine tensor element normal to the molecular plane of these molecules[3-6].

Clearly, optically detected magnetic resonance and ENDOR in zero field have been established as powerful methods for obtaining ^{14}N nuclear quadrupole and hyperfine interactions in excited triplet states.

In this communication we extend this method to other nuclei by reporting the first ^{35}Cl and ^{37}Cl nuclear quadrupole and hyperfine interactions in an excited state. Specifically, the zero field optical detection of the electron spin resonance[7] and $^{35,37}Cl$ ENDOR in the $^3(\pi,\pi^*)$ state of 8-chloroquinoline is observed and interpreted.

Experimental

The apparatus used is similar to that described previously[3]. The microwave field was applied through a rigid coaxial line to a helical slow wave structure[8] containing a crystal of durene doped with 10^{-3} m 8-chloroquinolin The RF field used to induce ENDOR transitions was applied by means of a "bridge T" constant resistance network in a Helmholtz arrangement. This method permits use of RF frequencies from less than 1 MHz to 50 MHz without adjustment. The entire setup was immersed in a liquid helium dewar which was pumped to a temperature of 1.7°K. The 3100 Å region of a 100 watt mercury short arc lamp served as the exciting source. The 0-0 band phosphorescence emission of 8-chloroquinoline was detected at a 90° angle to the exciting light and isolated by means of a 3/4 meter Jarrell-Ash Spectrometer equipped with a photomultiplier output.

Results

Two of the three electron transitions, those associated with the $\tau_y \rightarrow \tau_z$ and $\tau_x \rightarrow \tau_z$ electron spin manifolds, were observed with satisfactory resolution. The $\tau_y \rightarrow \tau_z$ multiplet is centered at 860 MHz while the $\tau_x \rightarrow \tau_z$ multiplet is centered at 3483 MHz. In both cases, under steady state exciting light conditions, the 0-0 band phosphorescence emission increased when the microwave field coupled the respective spin manifolds. At low microwave power (10 μ watts) the strong "allowed" electron transitions were found. As the microwave power was increased (100 μ watts) "forbidden" satellites split off the major transitions by ~ 3 MHz were

observed. At higher powers (100-1000μ watts) these "forbidden satellites saturated and an additional multiplet of satellites were observed split ~25-40MH from the center section. Figure 1 illustrates a microwave power study of the $\tau_x \rightarrow \tau_z$ transition. The same basic pattern was observed for the $\tau_y \rightarrow \tau_z$ transitions. ^{35}Cl and ^{37}Cl ENDOR were observed by monitoring the change in the phosphorescence intensity of the 0-0 band while saturating one of the $\tau_y \rightarrow \tau_z$ microwave transitions in the outer satellite multiplet and simultaneously sweeping the RF frequency. An example of an optically detected ^{35}Cl ENDOR in zero field is shown in Figure 2. All observed frequencies and relative intensities are given in TablesI,IV, and V. Measurement of the transition frequencies with an accuracy better than ~ 0.4 MHz was generally not possible due to the line widths associated with the individual lines (~ 1.0 MHz) and their overlap with other transitions.

Discussion

The structure of the zero field transitions $\tau_y \rightarrow \tau_z$ and $\tau_x \rightarrow \tau_z$ and the accompanying ENDOR observed in 8-chloroquinoline can be understood in terms of the spin Hamiltonian

$$\mathcal{H} = \mathcal{H}_{SS} + \mathcal{H}^{N}_{Q} + \mathcal{H}^{Cl}_{Q} + \mathcal{H}^{N}_{HF} + \mathcal{H}^{Cl}_{HF} \qquad (1)$$

where $\mathcal{H}_{SS}$ is the zero field splitting Hamiltonian

$$\mathcal{H}_{SS} = -(XS_x^{\,2} + YS_y^{\,2} + ZS_z^{\,2}), \qquad (2)$$

and $\mathcal{H}^{N}_{Q}$, $\mathcal{H}^{Cl}_{Q}$, and $\mathcal{H}^{N}_{HF}$, $\mathcal{H}^{Cl}_{HF}$ are the nuclear quadrupole interaction and electron-nuclear hyperfine interaction for nitrogen and chlorine.

Equation 1 may be simplified by the following assumptions. First, we assume that the y and z components of $\mathcal{H}^{N}_{HF}$ and $\mathcal{H}^{Cl}_{HF}$ may be neglected. This is justified in sofar as the EPR measurements of Maki, et al. on quinoline[9,10] have shown that $A_{xx} > A_{yy}, A_{zz}$ for the ^{14}N hyperfine interaction. Moreover, since the perturbations due to reasonable A_{yy} and A_{zz} components for either ^{14}N or $^{35,37}Cl$ would be much smaller than those due to A_{xx} they can, to a first approximation, be ignored. We will also assume that the principle axes of the tensor interactions $\mathcal{H}_{SS}$, $\mathcal{H}^{N}_{Q}$, and $\mathcal{H}^{Cl}_{Q}$, coincide. It is reasonable to assume that the principle axis of $\mathcal{H}^{N}_{Q}$ and $\mathcal{H}^{Cl}_{Q}$ would be close to the direction of the nitrogen lone pair orbital and along the C-Cl bond respectively (approximately along the Y molecular axis). Furthermore, in quinoline the nitrogen lone pair direction and the Y axis of $\mathcal{H}_{SS}$ are within a few degrees of each other[9,10]. We assume that 8-chloroquinoline does not deviate appreciably in this respect. With these approximations we can write

$$\mathcal{H}^{N}_{Q} = \sum_{k} \epsilon_k I_k^2 \qquad (k = x, y, z) \tag{3}$$

$$\mathcal{H}^{Cl}_{Q} = e^2 q(Cl) Q(Cl) \, [3m^2 - 15/4]/12 + \mathcal{H}^{Cl}_{Q}(\eta) \tag{4a}$$

$$\mathcal{H}^{Cl}_{Q}(\eta) = e^2 q(Cl) Q(Cl) \eta \, [I_+^2 + I_-^2]/24 \tag{4b}$$

$$\mathcal{H}^{N}_{HF} = A_{xx}(N) I_x S_x \tag{5}$$

$$\mathcal{H}^{Cl}_{HF} = A_{xx}(Cl)(1/2i)\ [I_+S_x - I_-S_x] \qquad (6)^{\dagger}$$

In order to simplify the discussion we will initially consider only ^{35}Cl.

The product functions $< u\ f\ v\ |^{\pm} = \tau_u\ \chi_f^{\pm}\ \chi_v$ form a set of eigenfunctions which diagonalize $\mathcal{H}_{SS}$, $\mathcal{H}^{N}_{Q}$ and $\mathcal{H}^{Cl}_{Q}$ $\left(\text{excluding } \mathcal{H}^{Cl}_{Q}(\eta)\right)$. τ_u, $\chi_f^{\pm}$ and χ_v are the electron, chlorine nuclear and nitrogen nuclear spin functions respectively. u and v correspond to x, y, and z while $\chi_f^{\pm}$ take on values + 3/2, -3/2, + 1/2, and -1/2. With this choice of basis functions, only $\mathcal{H}^{N}_{HF}$, $\mathcal{H}^{Cl}_{HF}$, and the parameter containing the Cl field gradient asymmetry, $\mathcal{H}^{Cl}_{Q}(\eta)$, are off diagonal in the Hamiltonian matrix. An energy level diagram appropriate to the $\tau_y \rightarrow \tau_z$ transition in 8-chloroquinoline is given in Figure 3. The zero field energies are arranged in the order $E_z > E_y > E_x$. The result of $\mathcal{H}^{Cl}_{Q}(\eta)$ is to mix states $< u\ f\ v\ |^{\pm}$ differing in $\Delta f = \pm 2$; thus, η cannot give intensity to "forbidden" transitions between the different spin manifolds. However, since $\mathcal{H}^{Cl}_{Q}(\eta)$ couples states that are also coupled to states in a different electron spin manifold by $\mathcal{H}^{Cl}_{HF}$, η may give rise to small frequency (~ 10 KHz) shifts and intensity variations via the interaction with $\mathcal{H}^{Cl}_{HF}$. Since these variations are very small, η cannot be obtained reliably from our data. Therefore, the ^{35}Cl first order nuclear quadrupole splitting between

---

† We have defined I_x as $1/2i\ [I^+ - I^-]$ rather than the conventional $1/2[I^+ + I^-]$. In our definition the Hamiltonian matrix is thus real so long as $A_{zz}(Cl)$ and $A_{yy}(Cl) = 0$. We could have reversed the molecular x and y axes and used the standard convention but we chose to have the axis system for quinoline[4,5] and 8-chloroquinoline the same.

$< Z\ 3/2|^{\pm}$ and $< Z\ 1/2\ |^{\pm}$, or $< Y\ 3/2\ |^{\pm}$, and $< Y\ 1/2\ |^{\pm}$ will be written in terms of one parameter $^{35}Q'$

$$^{35}Q' = e^2q(Cl)Q(^{35}Cl)(1 + \eta^2/3)^{1/2} \qquad (7)$$

The sign of $^{35}Q'$ was empirically found to be negative as would be expected from previous measurements of the chlorine quadrupole coupling constant in ground state molecules[11].

In the case of the nitrogen quadrupole interaction it has been shown[5] that in the approximation $A_{yy}(N)$, $A_{zz}(N) = 0$, $e^2qQ(^{14}N)$ and η cannot be obtained separately; therefore, we will use the measured parameter ν_- with the assumption that both the nitrogen asymmetry parameter, η, and $e^2qQ(^{14}N)$ are positive.

The principal result of $\mathcal{H}^{N}_{HF}$ acting as a perturbation is that the levels $< Z\ 3/2\ Z\ |^{\pm}$, $< Z\ 3/2\ Y\ |^{\mp}$, $< Z\ 1/2\ Z\ |^{\mp}$, and $< Z\ 1/2\ Y\ |^{\pm}$ shift to a higher energy by an amount $\alpha \simeq A^2_{xx}(N)/(Z-Y)$ and the levels $< Y\ 3/2\ Z|^{\mp}$, $< Y\ 3/2\ Y\ |^{\pm}$, $< Y\ 1/2\ Z|^{\pm}$, and $< Y\ 1/2\ Y\ |^{\mp}$ shift to lower energies by an equal amount (cf. Fig. 3). Similarly, the result of $\mathcal{H}^{Cl}_{HF}$ is to mix the states in the τ_y and τ_z manifolds. The order of the plus and minus sign, $< \ |^{\pm}$, corresponds to the components of Kramers pair which are not split in zero field. Table II list the states mixed under these perturbations. Because $\mathcal{H}^{Cl}_{HF}$ mixes states involving two or more basis states in the same electron spin manifold, $\mathcal{H}^{Cl}_{HF}$ cannot be adequately treated by first order perturbation theory. Therefore computer diagonalization of the Hamiltonian matrix was employed. It was found that under th perturbation $\mathcal{H}^{Cl}_{HF}$, the states shifted to a first approximation by energies relate to multiples of $\beta \simeq [A_{xx}(Cl)]^2/Z-Y$ (cf. Figure 3). An analysis

of the problem revealed that this approximation was good to within 0.3 MHz over a reasonable range of $A_{xx}(Cl)$ values. We should stress that this is only an approximation but is empirically[††] verified. Since we resolve no splittings in the spectra directly attributable to $\mathcal{H}^{Cl}_{HF}$, the β's are employed to treat $\mathcal{H}^{Cl}_{HF}$ as a "pseudo" first order perturbation.

From an inspection of the states mixed by $\mathcal{H}^{N}_{HF}$ and $\mathcal{H}^{Cl}_{HF}$ (cf. Table II) four types of transitions between the electron spin manifolds can be classified using the electron magnetic dipole moment transition operator. These can be described as: (a) electron spin transitions only, (b) simultaneous electron and nitrogen nuclear spin transitions, (c) simultaneous electron and chlorine nuclear spin transitions, and (d) simultaneous electron spin, and nitrogen and chlorine nuclear spin transitions. The approximate transition energies are given in Table I in terms of the spin Hamiltonian parameters. It should be noted that with the approximation A_{yy}, $A_{zz}(Cl, N) = 0$, the τ_x manifold is not mixed with τ_y or τ_z; thus, the basis functions $| X\ f\ v >^{\pm}$ are not perturbed. The primed states in the tables and figures correspond to the perturbed basis functions. With the above approximation it is immediately apparent from Table I that all parameters except $A_{xx}(Cl)$ can be obtained relatively easily and to reasonable accuracy. For example, $A_{xx}(N)$ can be estimated from the energy difference between the transitions $< Y\ 3/2\ X|' \rightarrow < Z\ 3/2\ X|'$ and the degenerate pair $< Y\ 3/2\ Z|'$: $< Y\ 3/2\ Y|' \rightarrow < Z\ 3/2\ Z|'$: $< Z\ 3/2\ Y|'$ while $\nu_-\ (^{14}N)$ can be obtained to a first approximation from the difference in

---

[††] The use of empirical connotes the observation of the shifts resulting in the computer diagonization of the Hamiltonian matrix over a range of $A_{xx}(Cl)$ values.

the transition energies $< Y\ 3/2\ Z|' \rightarrow < Z\ 3/2\ Y|'$ and $< Y\ 3/2\ Y|' \rightarrow < Z\ 3/2\ Z|'$. This region of the electron spin transitions $\tau_y \rightarrow \tau_z$ is shown in Figure 1 . In a similar fashion the ^{35}Cl field gradient parameter $^{35}Q'$ can be estimated from transitions associated with either the $\tau_x \rightarrow \tau_z$ or $\tau_y \rightarrow \tau_z$ manifolds. For instance, the transitions $< X\ 1/2\ X| \rightarrow < Z\ 3/2\ X|'$ and $< X\ 3/2\ X| \rightarrow < Z\ 1/2\ X|'$ or $< Y\ 1/2\ X|' \rightarrow < Z\ 3/2\ X|'$ and $< Y\ 3/2\ X|' \rightarrow < Z\ 1/2\ X|'$ may be used. In fact all parameters except $A_{xx}(Cl)$ can be obtained from many different combinations of transitions (cf. Table I). Table III lists the values and standard deviations obtained by averaging many of the different combinations possible in Table I. The difficulty in obtaining an accurate measurement of $A_{xx}(Cl)$ is reflected in the large error assigned to its value.

As in the cases of quinoline[4,5], quinoxaline[4] and 2,3-dichloroquinoxaline[3] optically detected ENDOR is predicted in 8-chloroquinoline. The intensity of the ENDOR transitions can be accounted for solely in terms of the electron magnetic dipole transition operator[5]. Thus, ENDOR is expected between nuclear levels in only the τ_y and τ_z manifold since the τ_x manifold is not mixed with other electron spin states within our approximations. Three different types of ENDOR are predicted and can be described as: (a) nitrogen nuclear spin transitions only, (b) chlorine nuclear spin transitions only, and (c) simultaneous chlorine and nitrogen nuclear spin transitions. In addition the ENDOR transitions should be associated with specific microwave transitions between the $\tau_y \rightarrow \tau_z$ or $\tau_x \rightarrow \tau_z$ manifolds. Table IV lists the observed ENDOR transition and assigns them to the classification and the associated microwave transition. Indeed all three types are observed and excellent agreement between the transition energies and associated microwave transitions is obtained. These data provide a

sensitive test of the uniqueness of the assignments made in Table I and the parameters used to obtain the transition energies.

Although we have dealt specifically with ^{35}Cl, we can explain and assign transitions associated with ^{37}Cl nuclear quadrupole and nuclear electron hyperfine interactions. The observed microwave transitions and assignments are listed in Table V along with the ENDOR transitions for the low frequency $\tau_y \rightarrow \tau_z$ microwave transitions.‡ Naturally the intensity of these transitions are a factor of three lower than the corresponding ^{35}Cl transition because of their relative isotopic abundance. Although the difference between the ^{35}Cl and ^{37}Cl nuclear quadrupole moment is clearly observed, the difference in the nuclear magnetic moment cannot be observed since the splittings arising from the chlorine hyperfine interaction is not sufficiently resolved.

The value of the chlorine coupling constant $e^2qQ(35)[1 - (\eta)^2/3]^{1/2} = 68.4$MHz is approximately the same as that reported for the ground state of 6-chloroquinoline (69.256MHz) and 7-chloroquinoline (69.362MHz)[12,13], indicating that in the π,π^* triplet state the electron environment of the chlorine nucleus is probably not changed significantly from that of the ground state.

---

‡ We have observed in 2,3-dichloroquinoxaline both the microwave transitions resulting from simultaneous electron spin and chlorine nuclear spin transitions and simultaneous electron spin and two chlorine nuclear spin transitions appearing as satellites split ~ 35 MHz and ~ 70 MHz respectively from the allowed electron spin transitions in both the 2|E| and D+|E| multiplets. In addition we have observed the ^{35}Cl and ^{37}Cl ENDOR. The chlorine interactions in this molecule might explain the intensity seen in transitions 2 and 7 and the small splitting observed in the ^{14}N ENDOR (Reference 3). This is currently being investigated.

Although our analysis of the observed spectra accounts for the major features of the data there are several minor discrepancies which cannot be understood within our approximations. First, it appears that we must consider finite $A_{yy}(N)$, $A_{zz}(N)$, $A_{yy}(Cl)$ and $A_{zz}(Cl)$ values to fit all transitions energies more accurately and to account for the lines widths. Secondly, at maximum power (cf. Figure 1(f)) six pairs of satellites appear in the $\tau_x \rightarrow \tau_z$ multiplet centered at ~ 3.339, 3.367, 3.373, 3.398, 3.404 and 3.431 GHz. These satellites may be due to ^{13}C or ^{1}H interactions or alternatively guest-host interactions. The possibilities should be distinguishable by isotope substitution and/or small Zeeman perturbations.

Acknowledgements: This work was supported by the Lawrence Radiation Laboratory (IMRD Division) under the auspices of the AEC. In addition we gratefully acknowledge D. V. Owens and M. A. El-Sayed (UCLA) for providing us with the samples.

References

(1) J. Schmidt and J. H. van der Waals, Chem. Phys. Letters, 2 (1968) 640.

(2) D. S. Tinti, M. A. El-Sayed, A. H. Maki and C. B. Harris, Chem. Phys. Letters, 3, 343 (1969).

(3) C. B. Harris, D. S. Tinti, M. A. El-Sayed and A. H. Maki, Chem. Phys. Letters 4, 409 (1969).

(4) I. Y. Chan, J. Schmidt, and J. H. van der Waals, Chem. Phys. Letters, 4, 269 (1969).

(5) M. J. Buckley, C. B. Harris, and A. H. Maki, Chem. Phys. Letters, 5, XXX (1970).

(6) J. Schmidt and J. H. van der Waals, Chem. Phys. Letters, 3, 546 (1969).

(7) The zero field parameters D and E were provided by D. V. Owens and M. A. El-Sayed, private communication.

(8) R. H. Webb, R. S. I., 33, 732 (1962).

(9) J. S. Vincent and A. H. Maki, J. Chem. Phys., 39, 3088 (1963).

(10) Y. Gondo and A. H. Maki, J. Chem. Phys., 50, 3270 (1969).

Table I.

Energies and Assignments of Observed Frequencies Involving Electron, ^{14}N, and ^{35}Cl Transitions.

Transition	Energy ‡	Observed Frequency (MHz)	Relative† Intensity	Classification
$\langle Y\ 3/2\ X\|' \rightarrow \langle Z\ 3/2\ X\|'$	$Z-Y+2\beta$	859.3	1.9	a
$\langle Y\ 1/2\ X\|' \rightarrow \langle Z\ 1/2\ X\|'$	$Z-Y+6\beta$			a
$\langle Y\ 3/2\ Z\|' \rightarrow \langle Z\ 3/2\ Z\|'$	$Z-Y+2\alpha+2\beta$	860.1	2.7	a
$\langle Y\ 3/2\ Y\|' \rightarrow \langle Z\ 3/2\ Y\|'$	$Z-Y+2\alpha+2\beta$			a
$\langle Y\ 1/2\ Z\|' \rightarrow \langle Z\ 1/2\ Z\|'$	$Z-Y+2\alpha+5\beta$			a
$\langle Y\ 1/2\ Y\|' \rightarrow \langle Z\ 1/2\ Y\|'$	$Z-Y+2\alpha+5\beta$			a
$\langle Y\ 3/2\ Z\|' \rightarrow \langle Z\ 3/2\ Y\|'$	$Z-Y-\nu_{-}+2\alpha+2\beta$	857.3	1.6	b
$\langle Y\ 1/2\ Z\|' \rightarrow \langle Z\ 1/2\ Y\|'$	$Z-Y-\nu_{-}+2\alpha+4\beta$			b
$\langle Y\ 3/2\ Y\|' \rightarrow \langle Z\ 3/2\ Z\|'$	$Z-Y+\nu_{-}+2\alpha+2\beta$	863.8	1.3	b
$\langle Y\ 1/2\ Y\|' \rightarrow \langle Z\ 1/2\ Z\|'$	$Z-Y+\nu_{-}+2\alpha+6\beta$			b
$\langle Y\ 3/2\ X\|' \rightarrow \langle Z\ 1/2\ X\|'$	$Z-Y-(Q'/2)+4\beta$	826.2	2	c
$\langle Y\ 3/2\ Y\|' \rightarrow \langle Z\ 1/2\ Y\|'$	$Z-Y-(Q'/2)+2\alpha+3\beta$			c
$\langle Y\ 3/2\ Z\|' \rightarrow \langle Z\ 1/2\ Z\|'$	$Z-Y-(Q'/2)+2\alpha+4\beta$			c
$\langle Y\ 1/2\ X\|' \rightarrow \langle Z\ 3/2\ X\|'$	$Z-Y+(Q'/2)+4\beta$	895.0	1.8	c
$\langle Y\ 1/2\ Z\|' \rightarrow \langle Z\ 3/2\ Z\|'$	$Z-Y+(Q'/2)+2\alpha+3\beta$			c
$\langle Y\ 1/2\ Y\|' \rightarrow \langle Z\ 3/2\ Y\|'$	$Z-Y+(Q'/2)+2\alpha+4\beta$			c
$\langle Y\ 3/2\ Z\|' \rightarrow \langle Z\ 1/2\ Y\|'$	$Z-Y-(Q'/2)-\nu_{-}+2\alpha+3\beta$	822.8	1.9	d
$\langle Y\ 3/2\ Y\|' \rightarrow \langle Z\ 1/2\ Z\|'$	$Z-Y-(Q'/2)+\nu_{-}+2\alpha+4\beta$	829.2	1.7	d
$\langle Y\ 1/2\ Z\|' \rightarrow \langle Z\ 3/2\ Y\|'$	$Z-Y+(Q'/2)-\nu_{-}+2\alpha+3\beta$	891.6	1.8	d
$\langle Y\ 1/2\ Y\|' \rightarrow \langle Z\ 3/2\ Z\|'$	$Z-Y+(Q'/2)+\nu_{-}+2\alpha+4\beta$	898.1	1.5	d

Table I. (continued)

Transition	Energy	Observed Frequency (MHz)	Relative† Intensity	Classification
$\langle X\ 3/2\ X\| \rightarrow \langle Z\ 3/2\ X\|'$	$Z-X+\beta$	3384.7	2.8	a
$\langle X\ 3/2\ Z\| \rightarrow \langle Z\ 3/2\ Z\|'$	$Z-X+\alpha+\beta$			a
$\langle X\ 3/2\ Y\| \rightarrow \langle Z\ 3/2\ Y\|'$	$Z-X+\alpha+\beta$			a
$\langle X\ 1/2\ X\| \rightarrow \langle Z\ 1/2\ X\|'$	$Z-X+3\beta$			
$\langle X\ 1/2\ Z\| \rightarrow \langle Z\ 1/2\ Z\|'$	$Z-X+\alpha+3\beta$			a
$\langle X\ 1/2\ Y\| \rightarrow \langle Z\ 1/2\ Y\|'$	$Z-X+\alpha+2\beta$			a
$\langle X\ 3/2\ Z\| \rightarrow \langle Z\ 3/2\ Y\|'$	$Z-X-\nu_{-}+\alpha+\beta$	3381.9	2	b
$\langle X\ 1/2\ Z\| \rightarrow \langle Z\ 1/2\ Y\|'$	$Z-X-\nu_{-}+\alpha+2\beta$			b
$\langle X\ 3/2\ Y\| \rightarrow \langle Z\ 3/2\ Z\|'$	$Z-X+\nu_{-}+\alpha+\beta$	3388.7	1.0	b
$\langle X\ 1/2\ Y\| \rightarrow \langle Z\ 1/2\ Z\|'$	$Z-X+\nu_{-}+\alpha+3\beta$			b
$\langle X\ 1/2\ X\| \rightarrow \langle Z\ 3/2\ X\|'$	$Z-X+(Q'/2)+\beta$	3419.5	2.1	c
$\langle X\ 1/2\ Z\| \rightarrow \langle Z\ 3/2\ Z\|'$	$Z-X+(Q'/2)+\alpha+\beta$			c
$\langle X\ 1/2\ Y\| \rightarrow \langle Z\ 3/2\ Y\|'$	$Z-X+(Q'/2)+\alpha+\beta$			c
$\langle X\ 3/2\ X\| \rightarrow \langle Z\ 1/2\ X\|'$	$Z-X-(Q'/2)+3\beta$	3350.8	2.8	c
$\langle X\ 3/2\ Z\| \rightarrow \langle Z\ 1/2\ Z\|'$	$Z-X-(Q'/2)+\alpha+3\beta$			c
$\langle X\ 3/2\ Y\| \rightarrow \langle Z\ 1/2\ Y\|'$	$Z-X-(Q'/2)+\alpha+2\beta$			c
$\langle X\ 1/2\ Y\| \rightarrow \langle Z\ 3/2\ Z\|'$	$Z-X+(Q'/2)+\nu_{-}+\alpha+\beta$	3422.7	.8	d
$\langle X\ 1/2\ Z\| \rightarrow \langle Z\ 3/2\ Y\|'$	$Z-X+(Q'/2)-\nu_{-}+\alpha+\beta$	3416.5	1.6	d
$\langle X\ 3/2\ Y\| \rightarrow \langle Z\ 1/2\ Z\|'$	$Z-X-(Q'/2)+\nu_{-}+\alpha+3\beta$	3354.3	1.2	d
$\langle X\ 3/2\ Z\| \rightarrow \langle Z\ 1/2\ Y\|'$	$Z-X-(Q'/2)-\nu_{-}+\alpha+2\beta$	3348.1	2.1	d

Table I. (continued)

‡ $\nu_- = 3\ e^2qQ(^{14}N)(1 - \eta/3)/4$; $Q' = e^2qQ(^{35}Cl)(1 - \eta^2/3)^{1/2}$.

† Relative within the same classification only.

[a] Electron spin transition.

[b] Simultaneous electron and nitrogen spin transition.

[c] Simultaneous electron and chlorine spin transition.

[d] Simultaneous electron, nitrogen, and chlorine spin transition.

Table II.

Basis States Mixed by $A_{xx}(N)$ and $A_{xx}(Cl)$

$A_{xx}(N)$

$$\{\langle Z\ 3/2\ Z|^{\pm},\quad \langle Y\ 3/2\ Y|^{\pm}\}$$
$$\{\langle Z\ 3/2\ Y|^{\pm},\quad \langle Y\ 3/2\ Z|^{\pm}\}$$
$$\{\langle Z\ 1/2\ Z|^{\pm},\quad \langle Y\ 1/2\ Y|^{\pm}\}$$
$$\{\langle Z\ 1/2\ Y|^{\pm},\quad \langle Y\ 1/2\ Z|^{\pm}\}$$

$A_{xx}(Cl)$

$$\{\langle Z\ 3/2\ X|^{\pm},\quad \langle Z\ 1/2\ X|^{\mp},\quad \langle Y\ 1/2\ X|^{\pm},\quad \langle Y\ 3/2\ X|^{\mp}\}$$
$$\left\{\begin{matrix}\langle Z\ 3/2\ Z|^{\pm}, & \langle Z\ 1/2\ Y|^{\pm}, & \langle Z\ 3/2\ Y|^{\mp}, & \langle Z\ 1/2\ Z|^{\mp} \\ \langle Y\ 3/2\ Y|^{\pm}, & \langle Y\ 1/2\ Z|^{\pm}, & \langle Y\ 1/2\ Y|^{\mp}, & \langle Y\ 3/2\ Z|^{\mp}\end{matrix}\right\}$$

$\langle\ |^{\pm}$ indicate Kramers Pairs

Table III

Spin Hamiltonian Values for 8-Chloroquinoline

Parameter	Value (MHz)	Standard Deviation (MHz)	Number of Combinations used from Table I;IV
X	-1970.0[a]	± 0.5	7
Y	555.5[a]	± 0.5	7
Z	1414.5[a]	± 0.5	7
$A_{xx}(N)$	19.5	± 1.0	3
$A_{yy}(N)$	b	-	-
$A_{zz}(N)$	b	-	-
$A_{xx}(Cl)$	15	-10, +15	12
$A_{yy}(Cl)$	b	-	-
$A_{zz}(Cl)$	b	-	-
$\nu_{-}(N)$	3.2	± 0.2	20
$Q'(^{35}Cl)$	-68.4	± 0.6	17

[a] Obtained from the D ± E and 2E convention such that $x + y + z = 0$.

[b] Data does not provide reliable values.

Table IV

Energies and Assignments of ^{14}N and ^{35}Cl ENDOR

ENDOR† Transition	Microwave Transition Saturated (MHz)	ENDOR‡ Energy	Observed ENDOR Frequency (MHz)	Relative Intensity	Classification
⟨Z 3/2 Y|'→ ⟨Z 3/2 Z|'		ν_-			a
⟨Z 1/2 Y|'→ ⟨Z 1/2 Z|'		$\nu_- + \beta$			a
⟨Y 3/2 Y|'→ ⟨Y 3/2 Z|'	857.3	ν_-	3.2	10	a
⟨Y 1/2 Y|'→ ⟨Y 1/2 Z|'		$\nu_- + \beta$			a
⟨Z 1/2 X|'→ ⟨Z 3/2 X|'		$(Q'/2)-2\beta$			b
⟨Z 1/2 Z|'→ ⟨Z 3/2 Z|'		$(Q'/2)-2\beta$			b
⟨Z 1/2 Y|'→ ⟨Z 3/2 Y|'		$(Q'/2)-\beta$			b
⟨Y 1/2 X|'→ ⟨Y 3/2 X|'	826.2	$(Q'/2)+2\beta$	33.5	11	b
⟨Y 1/2 Z|'→ ⟨Y 3/2 Z|'	822.8	$(Q'/2)+\beta$	33.9	2	b
⟨Y 1/2 Y|'→ ⟨Y 3/2 Y|'	829.2;826.2	$(Q'/2)+2\beta$	33.5	2;11	b
⟨Z 1/2 Z|'→ ⟨Z 3/2 Y|'		$(Q'/2)-\nu_--2\beta$			c
⟨Z 1/2 Y|'→ ⟨Z 3/2 Z|'		$(Q'/2)-\nu_--\beta$			c
⟨Y 1/2 Z|'→ ⟨Y 3/2 Y|'	829.2;826.2	$(Q'/2)-\nu_-+\beta$	31.5	2;2	c
⟨Y 1/2 Y|'→ ⟨Y 3/2 Z|'	822.8 ;826.2	$(Q'/2)+\nu_--2\beta$	37.5	7 ;2	c

Table IV (continued)

† We do not see ENDOR while saturating microwave transition in the $\tau_x \rightarrow \tau_z$ multiplet. Since ENDOR is not predicted in the τ_x manifold and presumably some relaxation mechanism interferes in the τ_z manifold, the observed ENDOR is assigned to the τ_y manifold.

‡ $\nu_- = 3e^2qQ(^{14}N)(1 - \eta/3)/4$; $Q' = e^2qQ(^{35}Cl)(1 - \eta^2/3)^{1/2}$.

a ^{14}N nuclear spin transition.

b ^{35}Cl nuclear spin transition.

c Simultaneous ^{14}N and ^{35}Cl nuclear spin transition.

Table V a.

Energies and Assignments of Observed Frequencies Involving Electron, ^{14}N, and ^{37}Cl Transitions.

Transition	Energy‡	Observed Frequency (MHz)	Relative† Intensity	Classification
$\langle Y\ 3/2\ X\|' \rightarrow \langle Z\ 1/2\ X\|'$	$Z-Y-(Q'/2)+4\beta$			a
$\langle Y\ 3/2\ Y\|' \rightarrow \langle Z\ 1/2\ Y\|'$	$Z-Y-(Q'/2)+2\alpha+3\beta$	833.0	1.5	a
$\langle Y\ 3/2\ Z\|' \rightarrow \langle Z\ 1/2\ Z\|'$	$Z-Y-(Q'/2)+2\alpha+4\beta$			a
$\langle Y\ 1/2\ X\|' \rightarrow \langle Z\ 3/2\ X\|'$	$Z-Y+(Q'/2)+4\beta$			a
$\langle Y\ 1/2\ Z\|' \rightarrow \langle Z\ 3/2\ Z\|'$	$Z-Y+(Q'/2)+2\alpha+3\beta$	887.9	1.3	a
$\langle Y\ 1/2\ Y\|' \rightarrow \langle Z\ 3/2\ Y\|'$	$Z-Y+(Q'/2)+2\alpha+4\beta$			a
$\langle Y\ 3/2\ Z\|' \rightarrow \langle Z\ 1/2\ Y\|'$	$Z-Y-(Q'/2)-\nu_{-}+2\alpha+3\beta$	829.2	1.7	b
$\langle Y\ 3/2\ Y\|' \rightarrow \langle Z\ 1/2\ Z\|'$	$Z-Y-(Q'/2)+\nu_{-}+2\alpha+4\beta$	835.9	1.1	b
$\langle Y\ 1/2\ Z\|' \rightarrow \langle Z\ 3/2\ Y\|'$	$Z-Y+(Q'/2)-\nu_{-}+2\alpha+3\beta$	884.1	1.9	b
$\langle Y\ 1/2\ Y\|' \rightarrow \langle Z\ 3/2\ Z\|'$	$Z-Y+(Q'/2)+\nu_{-}+2\alpha+4\beta$	891.6	1.5	b
$\langle X\ 1/2\ X\| \rightarrow \langle Z\ 3/2\ X\|'$	$Z-X+(Q'/2)+\beta$			a
$\langle X\ 1/2\ Z\| \rightarrow \langle Z\ 3/2\ Z\|'$	$Z-X+(Q'/2)+\alpha+\beta$	3412.0	1.9	a
$\langle X\ 1/2\ Y\| \rightarrow \langle Z\ 3/2\ Y\|'$	$Z-X+(Q'/2)+\alpha+\beta$			a
$\langle X\ 3/2\ X\| \rightarrow \langle Z\ 1/2\ X\|'$	$Z-X-(Q'/2)+3\beta$			a
$\langle X\ 3/2\ Z\| \rightarrow \langle Z\ 1/2\ Z\|'$	$Z-X-(Q'/2)+\alpha+3\beta$	3358.0	2.1	a
$\langle X\ 3/2\ Y\| \rightarrow \langle Z\ 1/2\ Y\|'$	$Z-X-(Q'/2)+\alpha+2\beta$			a
$\langle X\ 1/2\ Y\| \rightarrow \langle Z\ 3/2\ Z\|'$	$Z-X+(Q'/2)+\nu_{-}+\alpha+\beta$	3416.5	1.2	b
$\langle X\ 1/2\ Z\| \rightarrow \langle Z\ 3/2\ Y\|'$	$Z-X+(Q'/2)-\nu_{-}+\alpha+\beta$	3409.2	.8	b
$\langle X\ 3/2\ Y\| \rightarrow \langle Z\ 1/2\ Z\|'$	$Z-X-(Q'/2)+\nu_{-}+\alpha+3\beta$	3361.5	.8	b
$\langle X\ 3/2\ Z\| \rightarrow \langle Z\ 1/2\ Y\|'$	$Z-X-(Q'/2)-\nu_{-}+\alpha+2\beta$	3354.3	1.2	b

Table Vb.

Energies and Assignments of Observed Frequencies Involving Electron, ^{14}N, and ^{37}Cl Transitions.

ENDOR Transition	Microwave Transition Saturated (MHz)	ENDOR Energy‡	Observed ENDOR Frequency (MHz)	Relative† Intensity	Classification
$< Y\ 1/2\ X\|' \rightarrow < Y\ 3/2\ X\|'$	833.0	$(Q'/2)+2\beta$	26.8	1	c
$< Y\ 1/2\ Z\|' \rightarrow < Y\ 3/2\ Y\|'$	835.9	$(Q'/2)-\nu_{-}+\beta$	24.0	1	d
$< Y\ 1/2\ Y\|' \rightarrow < Y\ 3/2\ Z\|'$	829.2	$(Q'/2)+\nu_{-}-2\beta$	31.5	1	d

‡ $Q' = e^2qQ(^{37}Cl)(1 - \eta^2/3)^{1/2}$; $\nu_{-} = 3e^2qQ(^{14}N)(1 - \eta/3)$

† Relative within the same classification only.

a Simultaneous electron spin and ^{37}Cl nuclear spin transition.

b Simultaneous electron spin, ^{14}N, and ^{37}Cl nuclear spin transitions.

c ^{37}Cl nuclear spin transition.

d Simultaneous ^{37}Cl and ^{14}N nuclear spin transition.

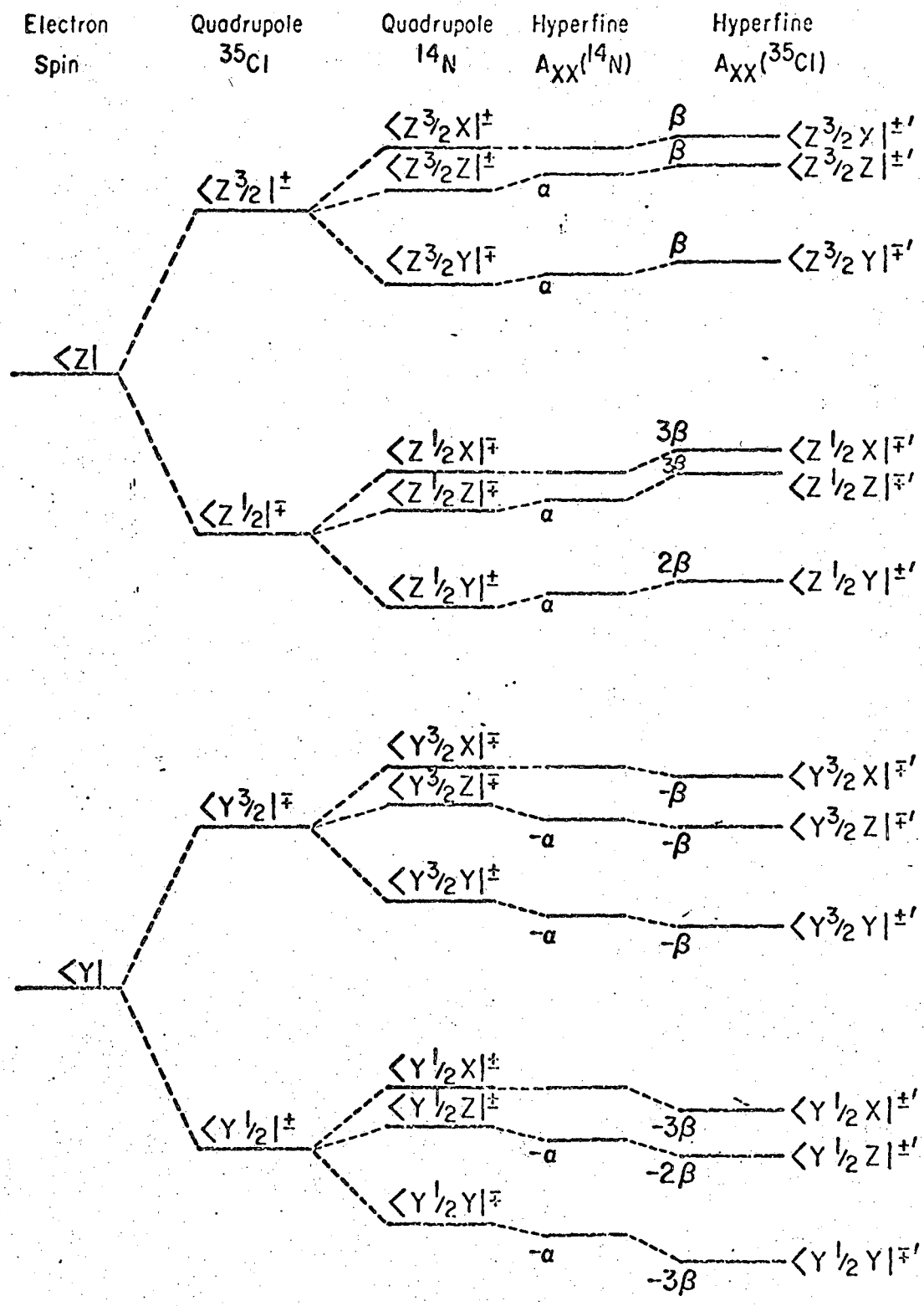

Figure 1. Optically detected microwave transitions in 8-chloroquinoline.

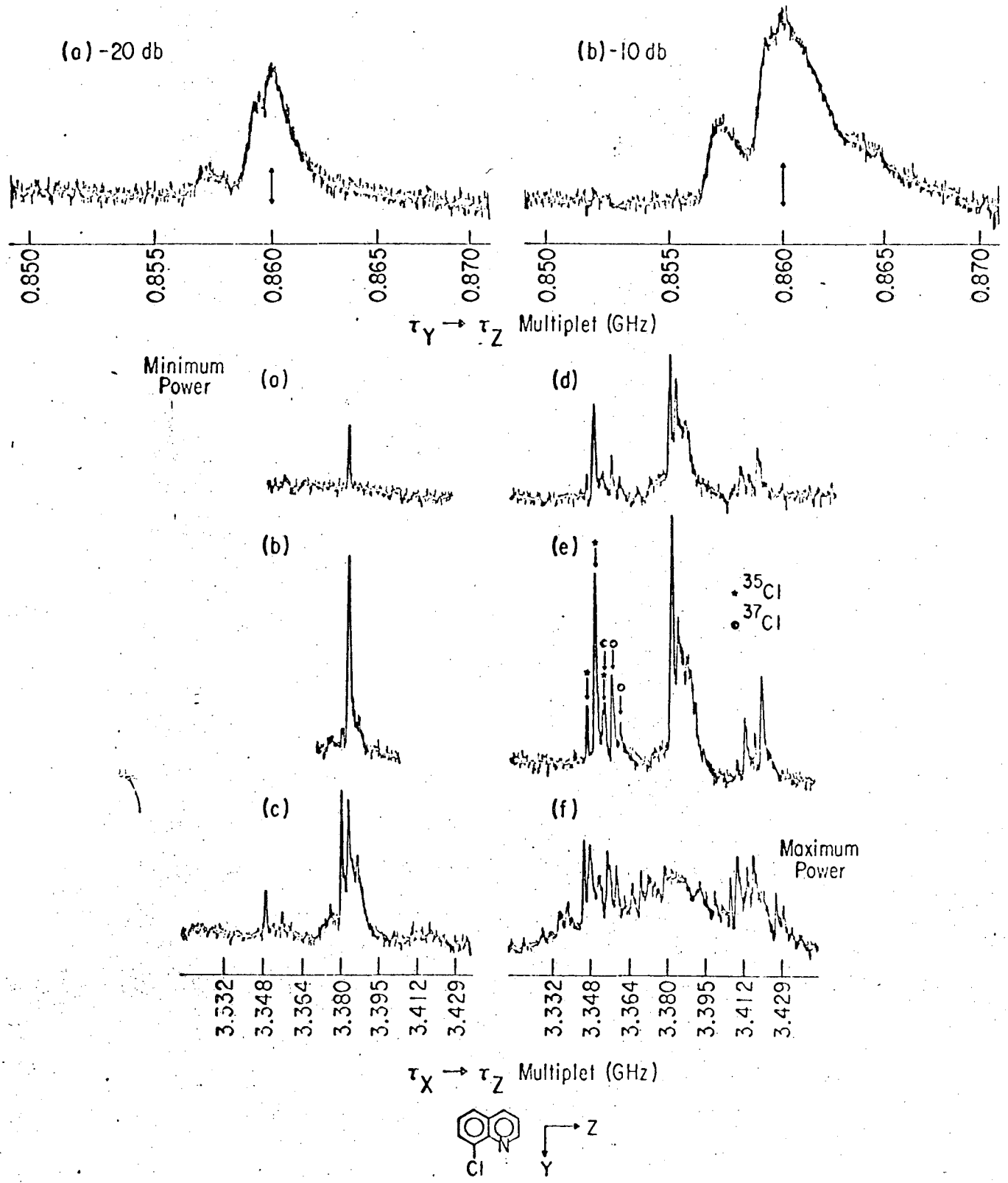

Figure 2. Optically detected ^{35}Cl ENDOR observed while saturating the microwave transitions at 826.2 MHz in the $\tau_y \rightarrow \tau_z$ multiplet. ENDOR transitions occur at ~ 37.5, ~33.5, and ~ 31.5 MHz (cf. Table IV).

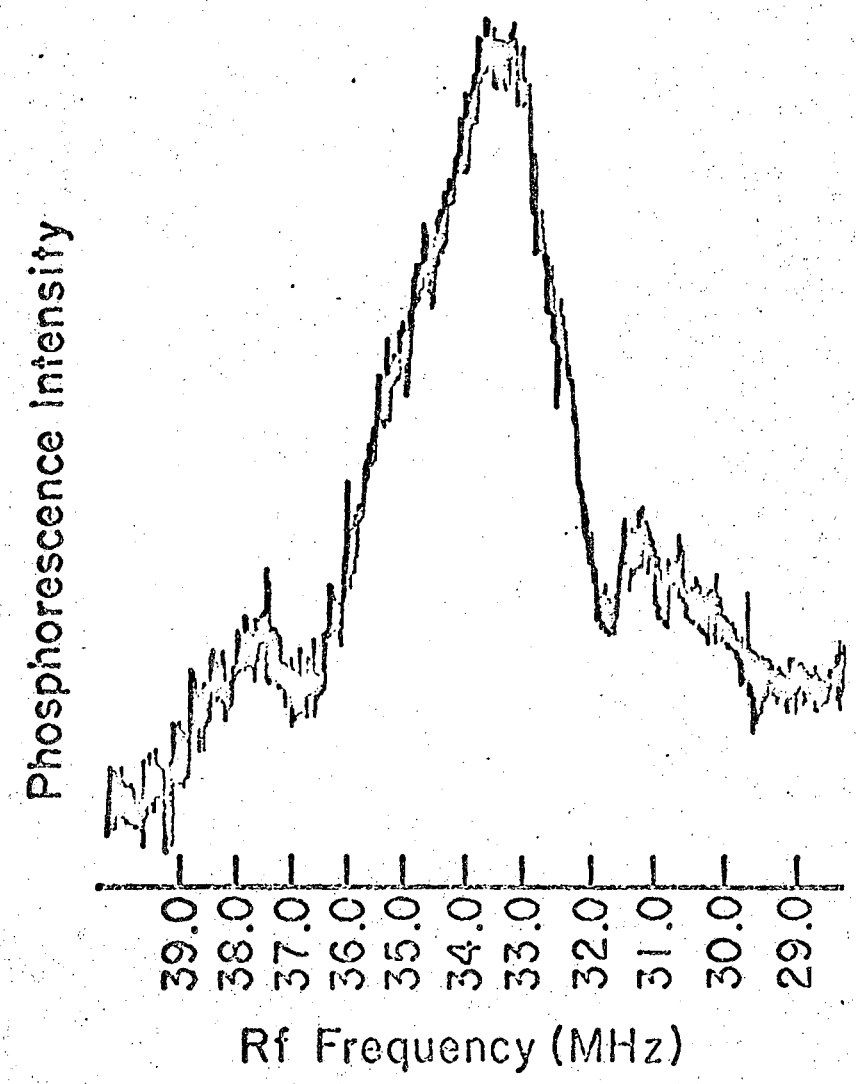

Figure 3. Energy level diagram for the τ_y and τ_z states.

LEGAL NOTICE

This report was prepared as an account of Government sponsored work. Neither the United States, nor the Commission, nor any person acting on behalf of the Commission:

A. Makes any warranty or representation, expressed or implied, with respect to the accuracy, completeness, or usefulness of the information contained in this report, or that the use of any information, apparatus, method, or process disclosed in this report may not infringe privately owned rights; or

B. Assumes any liabilities with respect to the use of, or for damages resulting from the use of any information, apparatus, method, or process disclosed in this report.

As used in the above, "person acting on behalf of the Commission" includes any employee or contractor of the Commission, or employee of such contractor, to the extent that such employee or contractor of the Commission, or employee of such contractor prepares, disseminates, or provides access to, any information pursuant to his employment or contract with the Commission, or his employment with such contractor.

TECHNICAL INFORMATION DIVISION
LAWRENCE RADIATION LABORATORY
UNIVERSITY OF CALIFORNIA
BERKELEY, CALIFORNIA 94720